



A chemical dynamics study on the gas-phase formation of triplet and singlet C₅H₂ carbenes

Chao He^{a,1}, Galiya R. Galimova^{b,c,1}, Yuheng Luo^{a,1}, Long Zhao^a, André K. Eckhardt^d, Rui Sun^{a,2}, Alexander M. Mebel^{b,2}, and Ralf I. Kaiser^{a,2}

^aDepartment of Chemistry, University of Hawai'i at Manoa, Honolulu, HI 96822; ^bDepartment of Chemistry and Biochemistry, Florida International University, Miami, FL 33199; ^cLaboratory of Combustion Physics and Chemistry, Samara National Research University, Samara 443086, Russia; and ^dInstitute of Organic Chemistry, Justus Liebig University, 35392 Giessen, Germany

Edited by Alexis T. Bell, University of California, Berkeley, CA, and approved October 14, 2020 (received for review September 15, 2020)

Since the postulation of carbenes by Buchner (1903) and Staudinger (1912) as electron-deficient transient species carrying a divalent carbon atom, carbenes have emerged as key reactive intermediates in organic synthesis and in molecular mass growth processes leading eventually to carbonaceous nanostructures in the interstellar medium and in combustion systems. Contemplating the short lifetimes of these transient molecules and their tendency for dimerization, free carbenes represent one of the foremost obscured classes of organic reactive intermediates. Here, we afford an exceptional glance into the fundamentally unknown gas-phase chemistry of preparing two prototype carbenes with distinct multiplicities—triplet pentadiynylidene (HCCCCCH) and singlet ethynylcyclopropenylidene (*c*-C₃H₂) carbene—via the elementary reaction of the simplest organic radical—methylidyne (CH)—with diacetylene (HCCCH) under single-collision conditions. Our combination of crossed molecular beam data with electronic structure calculations and quasi-classical trajectory simulations reveals fundamental reaction mechanisms and facilitates an intimate understanding of bond-breaking processes and isomerization processes of highly reactive hydrocarbon intermediates. The agreement between experimental chemical dynamics studies under single-collision conditions and the outcome of trajectory simulations discloses that molecular beam studies merged with dynamics simulations have advanced to such a level that polyatomic reactions with relevance to extreme astrochemical and combustion chemistry conditions can be elucidated at the molecular level and expanded to higher-order homolog carbenes such as butadiynylcyclopropenylidene and triplet heptatriynylidene, thus offering a versatile strategy to explore the exotic chemistry of novel higher-order carbenes in the gas phase.

reaction dynamics | molecular beams | trajectory calculations | electronic structure theory | carbenes

Since the pioneering discovery of the structural isomers cyclopropenylidene (*c*-C₃H₂, X¹A₁, **1**), vinylidenecarbene (H₂CCC, X¹A₁, **2**), and propargylene (HCCCH, X³B, **3**) (Fig. 1) in the laboratory and in extraterrestrial environments (1–9), the homologous series of the isomers C₃H₂ (**1** to **3**) and C₅H₂ (**4** to **6**) fascinated the physical (organic) and computational chemistry communities from the fundamental points of view of electronic structure and chemical bonding (10–12) as prototypes of highly unsaturated (partially) 2π-Hückel aromatics (**1** and **4**), singlet carbenes (**2** and **5**), and triplet diradicals (**3** and **6**). Cyclopropenylidene (**1**)—a three membered ring species of C_{2v} symmetry depicting an aromatic character and a carbene moiety at the apical carbon atom—represents the thermodynamically most stable C₃H₂ isomer. This molecule was first detected by Reisenauer et al. in low-temperature argon matrices (**3**) prior to its identification in a helium–acetylene gas discharge and toward the Taurus Molecular Clods (TMC-1) and the star-forming region Sagittarius B2 (Sgr B2) (**1**). The C_{2v} symmetric vinylidenecarbene (**2**) is linked to vinylidene (H₂CC; X¹A₁) by formally adding a carbon atom to the carbene moiety and can be produced via photolysis of propargylene (**3**) in an argon matrix at 10 K at 313 nm (**5**). Gas-phase vinylidenecarbene (**2**) was identified in a

helium–acetylene discharge (**13**) prior to its observation toward TMC-1 (**4**). Cyclopropenylidene (**1**) ring opens to propargylene (**3**) upon photoexcitation at 360 nm (**3**, **5**). The triplet multiplicity of the electronic ground state of the C₂ symmetric propargylene (**3**), in which each unpaired electron is formally located at each terminal carbon atom, leading to an unconventional 1,3-diradical, was recognized by Mebel et al., who computed the ground triplet ³B to lie 53 to 61 kJ·mol⁻¹ below the first excited singlet ¹A' state (14–16). Recent reaction dynamics studies provided compelling evidence that cyclopropenylidene (**1**) along with vinylidenecarbene (**2**) and/or propargylene (**3**) can be easily formed in the bimolecular gas-phase reactions of ground-state carbon atoms [C(³P)] with the vinyl radical [C₂H₃ (X²A')] (**17**) and of methylidyne [CH(X²Π)] with acetylene [C₂H₂(X¹Σ_g⁺)] (**18**).

Whereas a unified picture on the underlying chemistry and chemical bonding of the cyclopropenylidene (**1**)–vinylidenecarbene (**2**)–propargylene (**3**) system is beginning to emerge, gas-phase reaction dynamics studies sustaining a directed synthesis of distinct C₅H₂ isomers—ethynylcyclopropenylidene (*c*-C₃HCCCH, X¹A', **4**), pentatetraenylidene (H₂CCCCC, X¹A₁, **5**), and pentadiynylidene (HCCCCCH, X³Σ_g⁻, **6**) (Fig. 1)—are remarkably lacking. Ethynylcyclopropenylidene (**4**)—an ethynyl-substituted cyclopropenylidene (**1**)

Significance

Carbenes represent key reactive intermediates in molecular mass growth processes leading to carbonaceous nanostructures in the interstellar medium and in combustion systems. However, due to their short lifetimes and tendency for dimerization, carbenes represent one of the foremost obscured classes of reactive intermediates, with the preparation of carbenes in the gas phase remaining largely elusive. By merging molecular beams with electronic structure and quasi-classical trajectory calculations and exploiting triplet pentadiynylidene (HCCCCCH) and singlet ethynylcyclopropenylidene (*c*-C₅H₂) carbene as benchmarks, we present a versatile protocol to unravel the dynamics leading to exotic carbenes under single-collision conditions. These elementary mechanisms are of significance to our understanding of the fundamental processes leading to unsaturated organic transients in extreme, hydrocarbon-rich environments.

Author contributions: R.I.K. designed research; C.H., G.R.G., Y.L., L.Z., A.K.E., R.S., A.M.M., and R.I.K. performed research; C.H., G.R.G., Y.L., R.S., A.M.M., and R.I.K. analyzed data; and C.H., R.S., A.M.M., and R.I.K. wrote the paper.

The authors declare no competing interest.

This article is a PNAS Direct Submission.

Published under the PNAS license.

¹C.H., G.R.G., and Y.L. contributed equally to this work.

²To whom correspondence may be addressed. Email: ruisun@hawaii.edu, mebel@fiu.edu, or ralfk@hawaii.edu.

This article contains supporting information online at <https://www.pnas.org/lookup/suppl/doi:10.1073/pnas.2019257117/-DCSupplemental>.

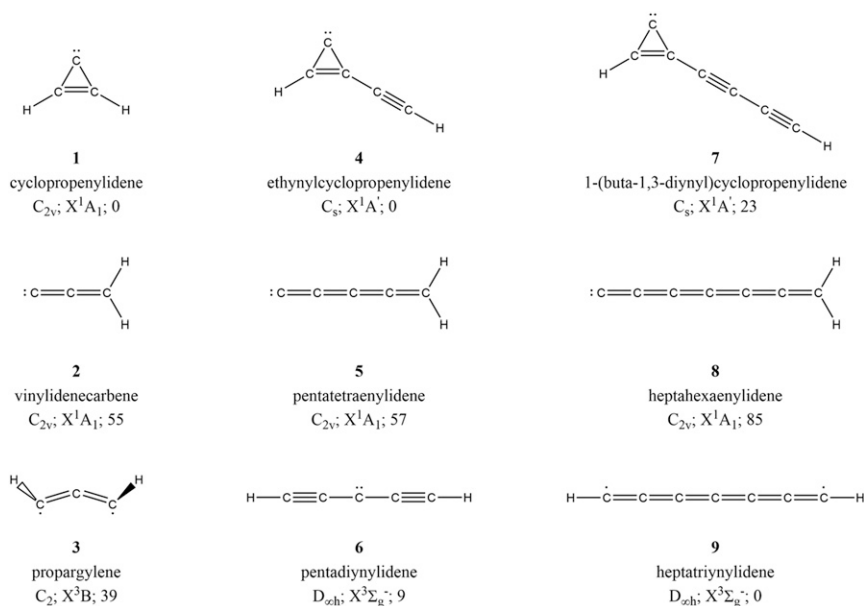


Fig. 1. Molecular structures, electronic states, point groups, and the relative energies of C_3H_2 (1 through 3), C_5H_2 (4 through 6), and C_7H_2 (7 through 9) isomers. Energies are shown in kilojoules per mole.

molecule with a C_s symmetry and a carbene moiety—signifies the thermodynamically most stable C_5H_2 isomer. Along with the C_{2v} symmetric cumulene carbene pentatetraenylidene (5), rotationally cold ethynylcyclopropenylidene (4) was detected in a helium-acetylene gas discharge via microwave spectroscopy (8, 19–23). Due to the absence of a permanent dipole moment, Maier et al. exploited electronic absorption spectroscopy to identify the linear pentadiynylidene molecule (6), which is classified as a carbene-centered diradical with a triplet ground state, in a 5-K neon matrix (24, 25). McMahan and coworkers prepared pentadiynylidene (6) in argon matrices at 10 K and solidified the assignment of a triplet molecular structure via infrared, ultraviolet-visible, and electron spin resonance spectra (26). Schwarz and coworkers employed negative ion chemical ionization mass spectroscopy in the gas phase to prepare pentatetraenylidene (5) and pentadiynylidene (6) (27). Very recently, thermally labile diazo precursors were employed to prepare pentadiynylidene (6) in a molecular beam (28). Overall, the replacement of a hydrogen atom in (1) and (3) by an ethynyl moiety leading to (4) and (6) not only reduces the energy difference between these isomer pairs from 39 to 9 $\text{kJ}\cdot\text{mol}^{-1}$ (8, 26) but also has a profound effect on the electronic structures of both triplet carbenes (3 and 6). This is reflected in the change from the C_2 to $D_{\infty h}$ point group and the switch from an 1,3- to a 3,3-diradical essentially located at the central carbon atom of pentadiynylidene (6) linking carbenes carrying two non-bonding electrons localized on a single carbon to quantum dot arrays and molecular electronic devices (29). However, despite evidence for the formation of (4) to (6) in low temperature matrices and in gas discharge processes, a directed gas-phase preparation of any C_5H_2 isomer has escaped chemists over the last decades. Therefore, contemplating the complexities of a directed gas-phase synthesis, short lifetimes of these transient molecules, and the tendency for dimerization (10, 26), free singlet and triplet carbenes ethynylcyclopropenylidene (4), pentatetraenylidene (5), and pentadiynylidene (6) represent one of the utmost obscured classes of organic transient molecules.

Here, we afford an exceptional glance into the fundamentally unknown gas-phase chemistry of two carbenes—singlet ethynylcyclopropenylidene (4) and triplet pentadiynylidene (6)—by exploring their preparation under single-collision conditions

through bimolecular reactions of the methylidyne radical (CH , $X^2\Pi$) with diacetylene (HCCCCH ; $X^1\Sigma_g^+$) via resonantly stabilized free 1- and 3-ethynylpropargyl radicals employing the crossed molecular beams method and merging these experimental studies with electronic structure calculations and molecular dynamics studies. The exploration of elementary reactions at the most fundamental, microscopic level conveys exclusive perceptions into the reaction mechanisms and underlying chemistry through which highly reactive carbenes such as the singlet ethynylcyclopropenylidene (4) and triplet pentadiynylidene (6) are formed without successive reactions in the gas phase. The coupling of experimental dynamics experiments with computational studies and trajectory simulations is very challenging for experiments and theory considering the polyatomic character of five heavy atoms along with the high dimensionality of this surface. This system is also appealing from the physical organic chemistry viewpoint to benchmark the chemical reactivity, bond-breaking processes, and the synthesis of hitherto elusive carbenes, which have remained undetected in interstellar and circumstellar environments, in single-collision events. Therefore, our strategy of combining crossed molecular beam studies by reacting two unstable reactants with *ab initio* and trajectory studies signifies a powerful template to unravel the elusive chemistry of reactive hydrocarbon species and to access a rather elusive class of highly unsaturated carbenes: singlet ethynylcyclopropenylidene (4) and triplet pentadiynylidene (6).

Results

Crossed Molecular Beam Studies: Laboratory Frame. The bimolecular reactions of electronically ground-state methylidyne(-d) radical (CH/CD , $X^2\Pi$) with diacetylene (HCCCCH ; $X^1\Sigma_g^+$) were conducted under single-collision conditions, exploiting a crossed molecular beam machine by intersecting supersonic beams of electronically ground-state methylidyne(-d) radical (CH/CD , $X^2\Pi$) with diacetylene (HCCCCH ; $X^1\Sigma_g^+$) perpendicularly at collision energies of 19.4 $\text{kJ}\cdot\text{mol}^{-1}$. Neutral reaction products were ionized via an electron impact ionizer (80 eV) within a triply differentially pumped quadrupole mass-spectrometric detector and then mass- and velocity-analyzed to record time-of-flight (TOF) spectra of the ionized products (*Materials and Methods*). The scattering signal for the elementary reaction of the methylidyne radical (CH ; $X^2\Pi$)

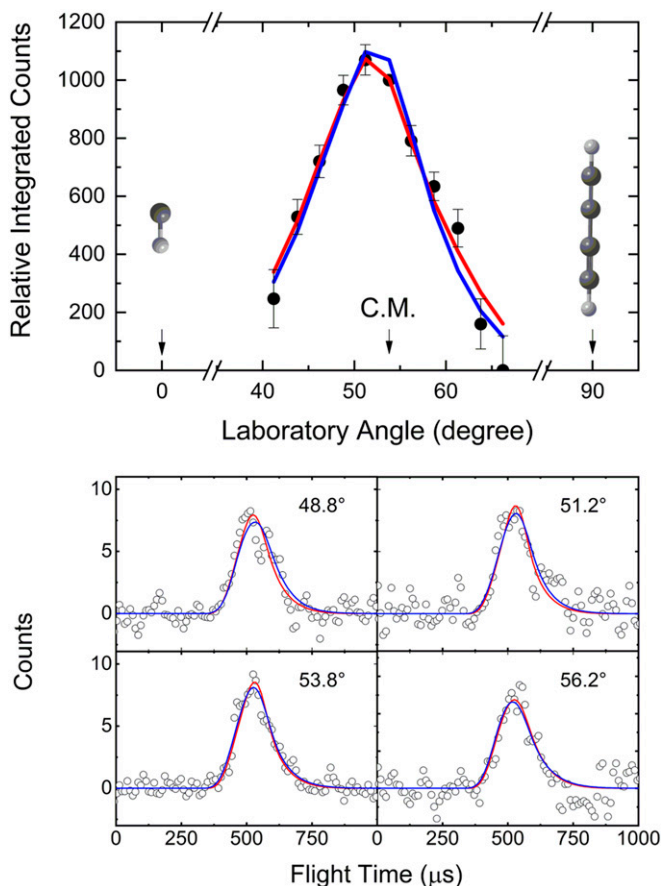
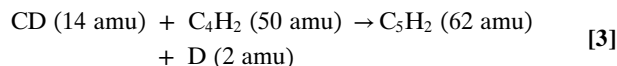
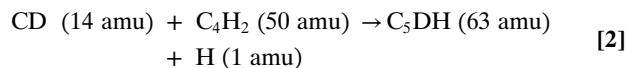
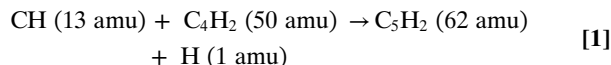


Fig. 2. Laboratory angular distribution (*Top*) and TOF spectra (*Bottom*) recorded at mass-to-charge ratio (m/z) of 62 for the reaction of the methylidyne radical (CH ; C_{cov} ; $X^2\Pi$) with diacetylene (HCCCCH ; D_{orb} ; $X^1\Sigma_g^+$). The directions of the methylidyne radical and diacetylene beams are defined as 0° and 90° , respectively. The red and blue solid lines represent the best fits exploiting CM functions depicted in Fig. 3 from the experimentally derived (red) and from the dynamics simulations (blue) with black circles defining the experimental data.

with diacetylene (HCCCCH ; $X^1\Sigma_g^+$) was observed at mass-to-charge ratios (m/z) of 62 (C_5H_2^+) and 61 (C_5H^+) with signal at $m/z = 62$ collected at a ratio of 1 ($m/z = 62$): 1.23 ± 0.02 ($m/z = 61$). These TOF spectra are superimposable after scaling, indicating a single reaction channel, namely the reaction of the methylidyne radical (CH ; 13 amu) with diacetylene (HCCCCH ; 50 amu), leading to the formation of C_5H_2 (62 amu) along with hydrogen atom (H ; 1 amu). The signal at $m/z = 61$ is associated with dissociative electron impact ionization of the neutral C_5H_2 product in the electron impact ionizer. These findings suggest that the C_5H_2 isomer(s) are formed via the methylidyne versus atomic hydrogen exchange channel upon reaction of methylidyne with diacetylene (reaction 1) with TOF spectra and the laboratory angular distribution (LAD) collected at $m/z = 62$. The LAD displays a maximum at 51.3° close to the center-of-mass (CM) angle of 53.8° and spans at least 27° in the laboratory frame (Fig. 2 and *SI Appendix*, Table S1). Since atomic hydrogen can be emitted from the methylidyne and/or from the diacetylene reactant, the outcome of the reaction of methylidyne-d with diacetylene (HCCCCH) was also explored (reactions 2 and 3). TOFs were recorded at the CM at $m/z = 63$ (C_5DH^+) and 62 ($\text{C}_5\text{D}^+/\text{C}_5\text{H}_2^+$). Signal was observed at both $m/z = 63$ and 62 (*SI Appendix*, Fig. S1); ion counts at $m/z = 62$ may also arise from dissociative electron impact ionization of C_5DH —if formed. Accounting for the ^{13}C isotopic contributions of 5.5% for five carbon atoms and

distinct recoil circles for atomic hydrogen versus deuterium loss, the ratio of the ion counts at $m/z = 63$ versus 62 is determined to be 1 ($m/z = 63$): 1.35 ± 0.04 ($m/z = 62$). This ratio does not match the ratio of $m/z = 62$ to $m/z = 61$ in the methylidyne–diacetylene system, suggesting that in the CD–diacetylene system both the hydrogen and the deuterium atoms are lost at a ratio of $2.98 \pm 0.86:1$ (*SI Appendix*, Fig. S1).



Crossed Molecular Beams Studies: CM Frame. The laboratory data alone offer explicit evidence on the gas-phase formation of C_5H_2 isomer(s) under single-collision conditions with the hydrogen atom emitted from the methylidyne and the diacetylene reactants. The prime directive of our studies is to unravel the nature of the C_5H_2 isomer(s) formed and the underlying reaction mechanism(s). This requires a transformation of the laboratory data into the CM reference frame resulting in the CM translational energy $P(E_T)$ and angular $T(\theta)$ flux distribution (Fig. 3). Within our error limits, the best-fit CM functions were obtained exploiting a single channel with the product mass combination of C_5H_2 (62 amu) plus H (1 amu). The maximum translational energy release (E_{max}) was derived from the $P(E_T)$ distribution to be $128 \pm 17 \text{ kJ}\cdot\text{mol}^{-1}$. Considering the principle of energy conservation, the E_{max} , collision energy (E_C), and the reaction energy ($\Delta_r G$) are connected via $E_{\text{max}} = E_C - \Delta_r G$ for those products born without internal excitation. Consequently, the reaction energy calculates to be $-109 \pm 17 \text{ kJ}\cdot\text{mol}^{-1}$. Further, the $P(E_T)$ distributions reveal a prominent distribution maximum slightly away from zero translational energy located at $10 \pm 5 \text{ kJ}\cdot\text{mol}^{-1}$, suggesting a loose exit transition state with only a minor rearrangement of the electron density. The average translational energy of the products was derived to be $33 \pm 4 \text{ kJ}\cdot\text{mol}^{-1}$, suggesting that only $26 \pm 4\%$ of the maximum energy is released into the translational degrees of freedom of the products. These findings propose indirect scattering dynamics involving C_5H_3 intermediate(s) undergoing unimolecular decomposition through loose exit transition state(s) via a simple bond-rupture process (30). Additional information on the reaction dynamics can be collected by inspecting the CM angular distribution $T(\theta)$. First, the $T(\theta)$ depicts flux over the complete angular range from 0° to 180° , proposing once again indirect scattering dynamics via complex formation and hence the existence of bound C_5H_3 intermediate(s). Second, the $T(\theta)$ portrays a forward scattering with an intensity ratio $I(0^\circ)/I(180^\circ)$ of about $(1.5 \pm 0.2):1.0$. These data suggest the existence of at least one channel involving an osculating complex, where a complex formation takes place, but the lifetime of the complex is too low to allow multiple rotations to complete (31, 32). The weak polarization of the $T(\theta)$ is the direct result of the inability of the light hydrogen atom to carry away (31) a significant fraction of the total angular momentum, which in turn leads to a significant rotational excitation of the final products.

Discussion

Energetics. To elucidate the intimate dynamics of the reaction of methylidyne radicals with diacetylene, we are merging the experimental data with electronic structure calculations and quasi-classical

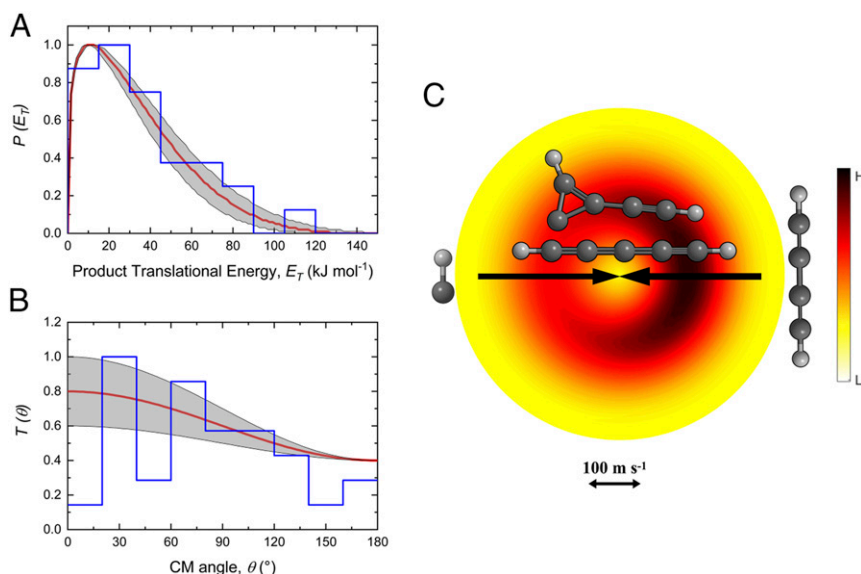


Fig. 3. CM distributions and the associated flux contour map. CM translational energy flux distribution (A), CM angular flux distribution (B), and the top view of their corresponding flux contour map (C) leading to the formation of ethynylcyclopropenylidene and pentadiynylidene plus atomic hydrogen in the reaction of methylidyne radical with diacetylene. Shaded areas indicate the error limits of the best fits accounting for the uncertainties of the laboratory angular distribution and TOF spectra, with the red solid lines defining the best-fit functions. The CM functions overlaid in blue are obtained from the dynamics simulations. The flux contour map represents the flux intensity of the reactive scattering products as a function of the CM scattering angle (θ) and product velocity (u). The color bar indicates the flux gradient from high (H) intensity to low (L) intensity. Colors of the atoms: carbon (light black) and hydrogen (gray).

trajectory studies (QCT). The electronic structure calculations reveal the existence of four energetically accessible C_5H_2 isomers **p1** to **p4** via atomic hydrogen loss (Fig. 4, Dataset S1, and SI Appendix, Fig. S2 and Table S2). These are ethynylcyclopropenylidene (**p1**, X^1A' , $\Delta_r G = -109 \pm 4 \text{ kJ mol}^{-1}$), pentadiynylidene (**p2**, $X^3\Sigma_g^-$, $\Delta_r G = -100 \pm 4 \text{ kJ mol}^{-1}$), pentatetraenylidene (**p3**, X^1A_1 , $\Delta_r G = -50 \pm 4 \text{ kJ mol}^{-1}$), and 2-cyclopropen-1-ylidenethenylidene (**p4**, X^1A_1 , $\Delta_r G = -28 \pm 4 \text{ kJ mol}^{-1}$). A comparison of these data with the experimentally derived reaction energy of $\Delta_r G = -109 \pm 17 \text{ kJ mol}^{-1}$ proposes that ethynylcyclopropenylidene (**p1**) and/or pentadiynylidene (**p2**) represent likely reaction products. At the present stage, we cannot eliminate contributions from **p3** and/or **p4** since these might be hidden in the low-energy section of the translational energy distribution. Therefore, our data support that at

least ethynylcyclopropenylidene (**p1**) and/or pentadiynylidene (**p2**) is/are formed under single-collision conditions. The order of energies for different C_5H_2 isomers calculated here at the CCSD(T)-F12/cc-pVTZ-f12 level (33, 34), **p1** (0 kJ mol^{-1}) < **p2** (9) < **p3** (59) < **p4** (81) closely agrees with the most accurate CCSDT(Q)/CBS (35) results, **p1** (0) < **p2** (3) < **p3** (57) < **p4** (84) (12), whereas earlier calculations gave a different result predicting ethynylcyclopropenylidene as the most stable structure: **p2** (0) < **p1** (8) < **p3** (58) < **p4** (88) (10, 12). Note that our calculations also elucidated a possible molecular hydrogen loss channel leading to pentynylidene (**p5**, $X^2\Pi$, $\Delta_r G = -124 \pm 4 \text{ kJ mol}^{-1}$); recall that within the sensitivity of our detection system no evidence for a molecular hydrogen loss channel was found.

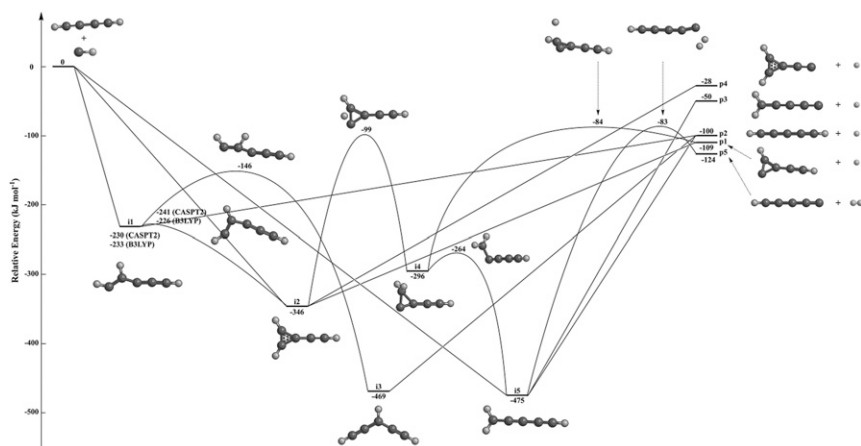


Fig. 4. Schematic representation of the potential energy surface of the reaction of the methylidyne radical with diacetylene. Energies calculated at the CCSD(T)-F12/cc-pVTZ-f12//B2PLYPD3/cc-pVTZ + ZPE(B2PLYPD3/cc-pVTZ) level (unless mentioned otherwise) are shown in kilojoules per mole and are relative to the energy of the separated reactants.

Electronic Structure Calculations. We would like to explore now the underlying reaction mechanism(s) leading to ethynylcyclopropenylidene (**p1**) and/or pentadiynylidene (**p2**). Our electronic structure calculations predict that the methylidyne radical can add barrierlessly to the π electron density of one of the carbon–carbon triple bonds of diacetylene, leading either to a C_s symmetric acyclic intermediate **i1** (X^2A') or to the cyclic collision complex **i2** (X^2B_1) with C_{2v} symmetry through addition to one of the terminal carbon atoms or to both carbon atoms of the acetylene moiety, respectively. The doublet radical intermediates **i1** and **i2** are stabilized by 230 and 346 $\text{kJ}\cdot\text{mol}^{-1}$ with respect to the separated reactants. At the B3LYP level of theory (36), a barrier of 7 $\text{kJ}\cdot\text{mol}^{-1}$ separates **i1** from **i2**. This barrier vanishes at the CASPT2 (37) level of theory, suggesting that if the collision complex **i1** exists at all it is metastable at most and isomerizes nearly instantaneously to **i2**. The wavefunction in the vicinity of **i1** features a significant multi-reference character as evidenced by a high value of the T1 diagnostic in CCSD(T)-F12 calculations exceeding 0.03. Therefore, we rely upon multireference CASPT2/cc-pVTZ energies for **i1** and the transition state from **i1** to **i2**. Moreover, **i1** could not be found as a local minimum at the B2PLYPD3/cc-pVTZ level; both **i1** and the transition state to **i2** could be optimized only at B3LYP/cc-pVTZ (38). These findings also point at a metastable character of **i1**. Note that **i2** can be rationalized as an ethynyl-substituted cyclopropenyl radical intermediate (C_{2v} point group) with all atoms residing within the molecular plane. This is quite distinct from the cyclopropenyl radical (C_3H_3), which alters the D_{3h} symmetry through vibronic coupling leading to a Jahn–Teller distorted C_s symmetric radical (39). Besides the addition of the methylidyne radical to the carbon–carbon triple bond leading to **i1** and/or **i2**, approach geometries to the acetylenic carbon–hydrogen bond can lead to a barrierless insertion of methylidyne forming the 1-ethynylpropargyl **i5** (X^2B_1) intermediate. Among these initial collision complexes, intermediate **i2** represents a key transient species. This complex may isomerize via a hydrogen shift from one of the C–H moieties of the cyclopropenylidene ring to the second C–H functional group, leading to a methylidyne unit (CH_2) along with a carbene at the ring by overcoming a barrier of 247 $\text{kJ}\cdot\text{mol}^{-1}$ to form intermediate **i4** (X^2A'). The latter can undergo ring opening to form 1-ethynylpropargyl **i5** (X^2B_1). This structure can be classified as a resonantly stabilized, ethynyl-substituted propargyl free radical intermediate and represents the global minimum of this section of the C_5H_3 potential energy surface. Finally, intermediate **i3** (X^2B_1)—the C_{2v} symmetric 3-ethynylpropargyl radical—can be accessed via [2,3] hydrogen migration in **i1**. Besides isomerization reactions, intermediates **i1** to **i5** may also undergo unimolecular decomposition. Here, the energetically favorable products ethynylcyclopropenylidene (**p1**) and pentadiynylidene (**p2**) can be formed via unimolecular decomposition of intermediates **i2/i4** and **i1/i3/i5**, respectively, through atomic hydrogen loss. With the exception of the pathway **i4** \rightarrow **p1** + H, which depicts a tight exit transition state located 25 $\text{kJ}\cdot\text{mol}^{-1}$ above the separated products, the alternative fragmentation pathways are barrierless and hence have loose exit transition states as reflected in simple C–H bond rupture processes. Also, the calculations identified two pathways to **p3** and **p4** via **i5** and **i2**, respectively. Note that the computationally predicted molecular hydrogen loss to **p5** requires a unimolecular decomposition of intermediate **i5** via a tight exit transition state located 41 $\text{kJ}\cdot\text{mol}^{-1}$ above the separated products.

Altogether, a connection of these results with our experimental data reveals interesting findings. First, a comparison of the computed with the experimental reaction energy for the atomic hydrogen loss pathway of $\Delta_r G = -109 \pm 17 \text{ kJ}\cdot\text{mol}^{-1}$ proposes that at least ethynylcyclopropenylidene (**p1**) and/or pentadiynylidene (**p2**) are formed via indirect scattering dynamics involving C_5H_3 collision complexes. This discloses that ethynylcyclopropenylidene (**p1**) and/or pentadiynylidene (**p2**) can be prepared in the gas phase as a result of a reaction between

two neutral species under controlled experimental conditions via a single-collision event with four pathways potentially linked to the formation of **p1** (**i1** \rightarrow **i2** \rightarrow **p1** + H; **i2** \rightarrow **p1** + H; **i1** \rightarrow **i2** \rightarrow **i4** \rightarrow **p1** + H; **i2** \rightarrow **i4** \rightarrow **p1** + H) and up to five to **p2** (**i1** \rightarrow **p2** + H; **i5** \rightarrow **p2** + H; **i1** \rightarrow **i2** \rightarrow **i4** \rightarrow **i5** \rightarrow **p2** + H; **i2** \rightarrow **i4** \rightarrow **i5** \rightarrow **p2** + H; **i1** \rightarrow **i3** \rightarrow **p2** + H). Second, reactions with CD expose two competing channels, atomic hydrogen and deuterium loss, with a ratio of a ratio of $2.02 \pm 0.08:1$. Third, a theoretically predicted molecular hydrogen loss to **p5** was not observed experimentally, most likely due to the tight exit transition state from **i5** to **p5**, which is located above the energy of the separated reactants.

Reaction Dynamics Simulations. These open queries mandate QCT calculations, thus bridging the dynamics experiments with the theoretical understanding of the methylidyne–diacetylene system. These trajectory studies reveal exciting results and deliver compelling evidence on the formation of both singlet ethynylcyclopropenylidene (**p1**) and triplet pentadiynylidene (**p2**). The low reaction probability of less than 5% for all impact parameters makes the dynamics simulations very expensive. It is important to note that, although carefully calibrated (*SI Appendix, Table S3*), a single reference method such as B3LYP/cc-pVDZ employed in this QCT study could potentially suffer from representing structures of multireference character and, more generally, the density functional theory (DFT) method is less accurate than the highly correlated CCSD(T)-F12/cc-pVQZ-f12 method. Nevertheless, this compromise is inevitable because of the load of the computation: over 12 million energy gradient calculations are required to propagate more than 1,000 trajectories. Overall, the reaction probability accounts for addition and insertion channels (Fig. 5 and *Movies S1–S8*) as anticipated from ab initio calculations, holds a maximum at an impact parameter of 100 PM, and decreases to zero at 500 PM (*SI Appendix, Fig. S3*). The local maximum at 400 PM represents the optimal insertion distance into the carbon–hydrogen bond of diacetylene leading to collision complex **i5** (*Movie S6* and *S7*); representative trajectories depicting an addition of methylidyne to the terminal carbon of diacetylene leading to **i1** and cycloaddition to the carbon–carbon triple bond forming **i2** are visualized in *Movies S1–S5*, respectively. First, less than a quarter of trajectories involving addition of methylidyne to a single-carbon atom pass through short-lived (21 fs) collision complex **i1**. Among these trajectories, 43% isomerize to **i2** leading to singlet ethynylcyclopropenylidene (**p1**) via **i1** \rightarrow **i2** \rightarrow **p1** + H (*Movie S1*); 29% undergo several isomerization to eventually form **i5** and then produce triplet pentadiynylidene (**p2**) via **i1** \rightarrow **i2** \rightarrow **i1** \rightarrow **i5** \rightarrow **p2** + H (*Movie S2*) via hydrogen atom loss from the diacetylene reactant. It should be noted that there is no saddle point connecting intermediates **i1** and **i5**. Instead of having a 1,2-H shift to occur to produce **i5** from **i1**, the system prefers to close the three-member ring to **i2**, then the hydrogen shift happens to **i4** followed by ring opening to **i5**. So, instead of the **i5** \rightarrow **i1** path, the minimal energy path follows **i1** \rightarrow **i2** \rightarrow **i4** \rightarrow **i5**. The reason for that is instability of **i1** with respect to the ring closure to **i2**. The absence of the saddle point does not mean that there could not be trajectories from **i1** to **i5**; in dynamics, the system does not have to go through a saddle point from one minimum to another (40). Fourteen percent of trajectories isomerize to **i2** and then isomerize back to **i1**, also leading to triplet pentadiynylidene (**p2**) via **i1** \rightarrow **i2** \rightarrow **i1** \rightarrow **p2** + H (*Movie S3*); the remaining trajectories (14%) involve decomposition of **i1** to triplet pentadiynylidene (**p2**) and a hydrogen atom ejection from the diacetylene reactant (*Movie S4*). Second, trajectories following cycloaddition to **i2** isomerize eventually forming triplet pentadiynylidene (**p2**) via **i2** \rightarrow **i1** \rightarrow **i5** \rightarrow **p2** + H with the hydrogen atom ejected from the methylidyne reactant (*Movie S5*). Third, the remaining trajectories involving insertion collision complex **i5** dissociate to triplet pentadiynylidene (**p2**) via **i5** \rightarrow **p2** + H

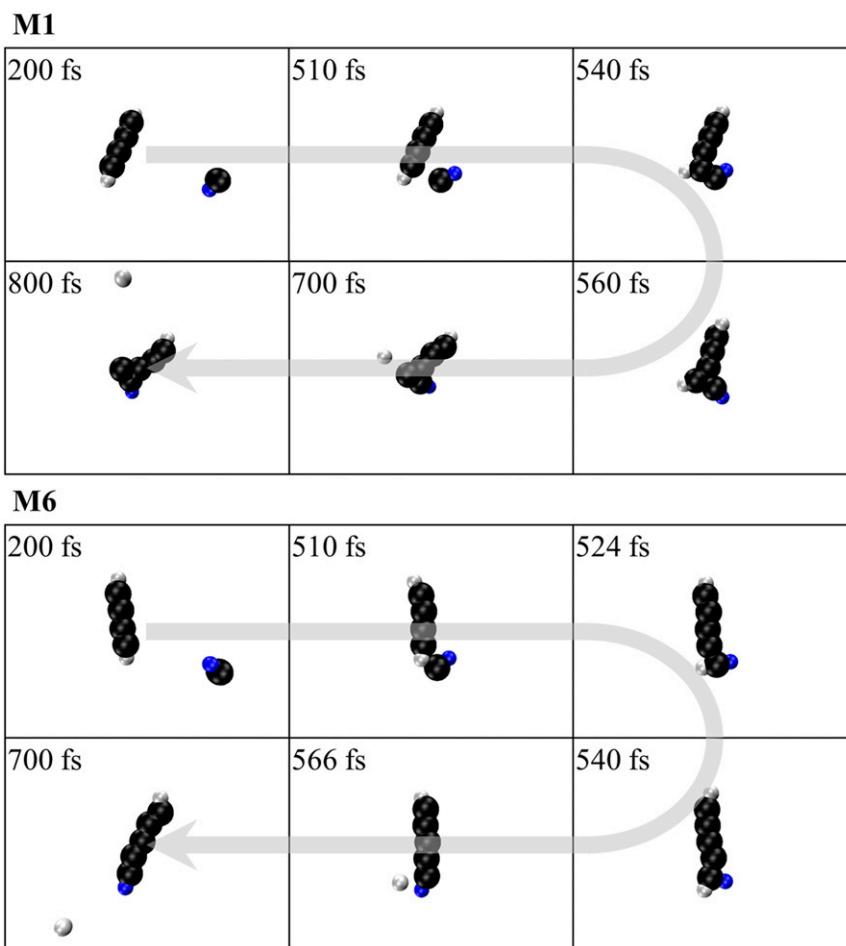


Fig. 5. Snapshots of representative trajectories from the dynamics simulations leading to singlet ethynylcyclopropenylidene (**p1**, *Top*) and triplet pentadiynylidene (**p2**, *Bottom*). A complete set of movies representing all reaction pathways can be seen in [Movies S1–S8](#). Carbon atoms are color-coded in black, whereas hydrogen atoms of diacetylene and methylidyne are colored in gray and blue, respectively.

with the hydrogen atoms ejected from the diacetylene (86%) ([Movie S6](#)) and methylidyne (14%) reactants ([Movie S7](#)), respectively. These hydrogen atom losses dominate the reactive trajectories ($94 \pm 5\%$), with $89 \pm 8\%$ of the trajectories leading to triplet pentadiynylidene (**p2**) and $11 \pm 4\%$ to singlet ethynylcyclopropenylidene (**p1**); note that no trajectories leading to the higher energy isomers **p3** or **p4** are observed. It is educational to compare these branching ratios with those obtained from statistical (RRKM, Rice–Ramsperger–Kassel–Marcus) (41) calculations ([SI Appendix](#)). Within the limit of an RRKM treatment, the total available energy is assumed to be completely redistributed within the internal vibrational degrees of freedom of the reaction intermediates. RRKM branching ratios were predicted to yield predominantly triplet pentadiynylidene (**p2**) (79%) and singlet ethynylcyclopropenylidene (**p1**) (20%), with the remaining channels leading to **p3**, **p4**, and **p5** contributing less than 1% ([SI Appendix](#)). Therefore, both RRKM and ab initio molecular dynamics (AIMD) simulations correlate nicely, predicting the predominant formation of triplet pentadiynylidene (**p2**) and singlet ethynylcyclopropenylidene (**p1**) albeit with higher yields of triplet pentadiynylidene (**p2**) in the trajectory calculations. This may suggest that the reaction is not completely statistical as evident, for example, from the very short lifetimes of the collision complex **i1** isomerizing to **i5**. Also, the trajectory calculations also allow us to trace the hydrogen atoms at the methylidyne and diacetylene reactants. The AIMD simulations observe both atomic hydrogen loss from the diacetylene and methylidyne reactants at a ratio of ($7 \pm$

1):1, that is, a preference of the hydrogen emission from the diacetylene reactant. To a minor amount, $6 \pm 4\%$ of trajectories lead to molecular hydrogen loss from **i5** through a tight exit transition state via $\mathbf{i5} \rightarrow \mathbf{p5} + \text{H}_2$ ([Movie S8](#)). Recall that no molecular hydrogen loss was observed experimentally; the theoretically predicted fraction is below the detection limit in our experiment.

Finally, it is interesting to compare the CM functions obtained from the dynamics simulations with those derived from fitting the experimental data ([Fig. 3](#)). Considering the CM angular distribution, the dynamics simulations predict a nearly isotropic, slightly forward scattering in agreement with the experiments. The predicted maximum energy release as derived from the CM translational energy distribution of the trajectory simulations of $116 \text{ kJ}\cdot\text{mol}^{-1}$ agrees well with the experimentally derived value of $128 \pm 17 \text{ kJ}\cdot\text{mol}^{-1}$; likewise, the experimentally derived distribution maximum of $10 \pm 5 \text{ kJ}\cdot\text{mol}^{-1}$ is near the $23 \pm 8 \text{ kJ}\cdot\text{mol}^{-1}$ obtained from the AIMD simulations. As a matter of fact, the CM functions derived from the dynamics simulations fit the TOF data and the laboratory angular distribution exceptionally well ([Fig. 2](#)), revealing that dynamics calculations of complex systems such as for the methylidyne–diacetylene reaction have reached a level of sophistication to predict the chemical dynamics of complex, multiatomic systems quantitatively, bespeaking the validity of AIMD with B3LYP/cc-pVDZ in representing this specific reaction. Nonetheless, in a general case, the AIMD/DFT simulations, although providing insightful movies ([Movies S1–S8](#)) and mechanisms, should mostly be considered as a qualitative representation of the considered

reactions of similar complexity unless the results could be verified by experiments as demonstrated here.

Conclusions

Our combined experimental and theoretical investigations provided compelling evidence on the formation of singlet ethynylcyclopropenylidene (**p1**, X^1A') and triplet pentadiynylidene carbene (**p2**, $X^3\Sigma_g^-$) under single-collision conditions via the elementary reaction of a methylidyne radical with diacetylene in the gas phase involving indirect scattering dynamics. Our studies revealed that the reaction has no entrance barrier, all barriers involved in the formation of ethynylcyclopropenylidene and pentadiynylidene are well below the energy of the separated reactants, and the overall reactions to prepare both isomers are exoergic. Electronic structure and quasiclassical trajectory calculations further identified three (resonantly stabilized) reaction intermediates on the doublet surface: metastable ethenylpropargylene (**i1**, X^2A'), 1-ethynylcyclopropenyl (**i2**, X^2B_1), and 1-ethynylpropargyl (**i5**, X^2B_1). The chemical dynamics leading to the gas-phase preparation of ethynylcyclopropenylidene (**p2**, **4**) and pentadiynylidene (**p1**, **6**)—classified as higher homologous molecules of cyclopropenylidene (**1**) and propargylene (**3**) (Fig. 1)—are relevant to combustion and astrochemical regimes. In combustion systems, the inherent C_5H_3 potential energy surface is of fundamental importance for several key reactions, where successive reactions between any C_5H_3 isomer with methyl radicals (CH_3) can access multiple C_6H_6 isomers (42–44)—among them the aromatic benzene molecule, which represents the basic molecular building block of polycyclic aromatic hydrocarbons. In deep space, both methylidyne radicals along with polyacetylenes like diacetylene (C_4H_2) and triacetylene (C_6H_2) have been detected toward the carbon-rich protoplanetary nebula CRL 618 via infrared spectroscopy (45, 46). Therefore, both ethynylcyclopropenylidene (**p1**) and pentadiynylidene carbene (**p2**) are expected to be formed toward CRL 618 via bimolecular gas-phase reactions of methylidyne with diacetylene. Considering the $D_{\infty h}$ symmetry, pentadiynylidene carbene lacks a permanent dipole moment and, hence, can only be identified in deep space by infrared spectroscopy. This finding contrasts molecular structure of the C_s symmetric ethynylcyclopropenylidene isomer, which has a dipole moment of 3.5 Debye (47) and, therefore, can be searched for with radio telescopes.

The exploration of the chemical dynamics leading to the preparation of exotic singlet and triplet carbenes in the gas phase has just scratched the surface. The reaction mechanisms extracted here do not only highlight the critical needs of fundamental reaction dynamics studies relevant to the formation of carbenes and the carbon budget in extreme environments but can be applied to predict the formation and guide the search for unusual carbenes like butadiynylcyclopropenylidene (**7**, X^1A'), heptahexaenylydene (**8**, X^1A_1), and heptatriynylidene (**9**, $X^3\Sigma_g^-$) in combustion systems and in the interstellar medium (Fig. 1) (9, 11, 22, 25, 48–50). Formally replacing one of the hydrogen atoms of cyclopropenylidene (**1**) by a linear butadiynyl moiety leads to butadiynylcyclopropenylidene (**7**) (11). This singlet carbene was first observed in an electrical discharge of diacetylene in neon via Fourier-transform microwave spectrometer (48). Heptahexaenylydene (**8**) was first prepared through charge stripping of the corresponding radical anion and detected via microwave spectroscopy (49, 51). With dipole moments exceeding 7 Debye, these isomers were proposed as ideal candidates for astronomical searches (19, 25). The microwave inactive triplet heptatriynylidene (**9**) (11) was probed in neon matrices via its electronic absorption spectra through the $^3\Sigma_u^- \leftarrow X^3\Sigma_g^-$ transition and also characterized by cavity ring down spectroscopy (50, 52). The combined experimental and theoretical results as provided here lead us to predict that both butadiynylcyclopropenylidene (**7**) and heptatriynylidene (**9**) could be prepared in the gas

phase not only in the laboratory, but also in the interstellar medium and in combustion flames via the elementary reaction of the methylidyne radical with triacetylene (C_6H_2). An understanding of the synthesis of highly reactive singlet and triplet carbenes will rely on critical combination of gas-phase molecular beams experiments under single-collision conditions combined with electronic structure and dynamics calculations as achieved here, thus closing the gap between (astronomical) observational and laboratory data on the exotic hydrocarbon chemistry that has existed for decades. The excellent agreement between fundamental experimental dynamics studies under single-collision conditions and the outcome of trajectory simulations reveals that molecular beams studies merged with AIMD simulations have advanced to such a level that complex, polyatomic reactions with exceptional relevance to extreme astrochemical (interstellar medium, atmospheres of planets and their moons) and combustion chemistry conditions can be explored from the fundamental chemical dynamics viewpoint.

Materials and Methods

Experimental. The reactions of the methylidyne (CH , $X^2\Pi$) and CD ($X^2\Pi$) radicals with diacetylene ($HCCCCH$; $X^1\Sigma_g^+$) were studied under single-collision conditions utilizing a crossed molecular beams machine at the University of Hawaii (53). In the primary source chamber, the pulsed supersonic methylidyne beam was generated via photodissociation (COMPex 110, 248 nm, 30 Hz; Coherent, Inc.) of helium-seeded (99.9999%; AirGas) bromoform ($CHBr_3$; Aldrich). After passing through the skimmer, the methylidyne radical beam was velocity-selected by a four-slot chopper wheel yielding a peak velocity v_p of $1,835 \pm 23 \text{ m}\cdot\text{s}^{-1}$ and a speed ratio S of 12.2 ± 1.3 (SI Appendix, Table S1). Laser-induced fluorescence determined the rotational temperature of the methylidyne radicals to be $14 \pm 1 \text{ K}$ (54). In the secondary source chamber, a section of the supersonic diacetylene beam defined by $v_p = 630 \pm 15 \text{ m}\cdot\text{s}^{-1}$ and $S = 23.2 \pm 0.3$ seeded at a level of 5% in argon (99.9999%; AirGas) crossed perpendicularly with the section of the methylidyne radical beam, resulting in a collision energy (E_c) of $19.4 \pm 0.4 \text{ kJ}\cdot\text{mol}^{-1}$ and a CM angle (Θ_{CM}) of $53.8 \pm 0.3^\circ$. Diacetylene was synthesized according to a literature procedure (55). Each gas pulse was released by a piezoelectric pulse valve operated at a repetition rate of 60 Hz and pulse width of 80 μs with the secondary pulsed valve 88 μs prior to the primary pulsed valve. For the corresponding isotopic substitution experiments of CD , bromoform- d ($CDBr_3$, >99.5%; Aldrich) acted as a precursor; the pulse of the primary beam was characterized through $v_p = 1,810 \pm 27 \text{ m}\cdot\text{s}^{-1}$ and $S = 12.2 \pm 0.9$, resulting in $E_c = 20.1 \pm 0.4$ and $\Theta_{CM} = 51.8 \pm 0.3^\circ$ (SI Appendix, Table S1). Reactively scattered products were sampled via a triply differentially pumped mass spectrometric detector (quadrupole mass spectrometer, QMS), which is rotatable in the plane defined by both supersonic beams. The neutral reaction products entering the detector at pressures of typically 5×10^{-12} Torr were ionized in the electron impact ionizer at 80 eV and filtered according to mass-to-charge ratio (m/z) in the QMS (QC 150; Extrel); the ions are collected by a Daly-type ion counter. Up to 5.4×10^5 TOF spectra were recorded at laboratory angles between 30° and 69° with respect to the methylidyne beam at each angle. A forward-convolution method is applied to convert the laboratory data into the CM frame yielding the CM translational energy $P(E_T)$ and angular $T(\theta)$ flux distributions. These functions comprise the reactive differential cross-section $I(\theta, u)$ at CM scattering angle θ and CM velocity u , $I(u, \theta) \sim P(u) \times T(\theta)$. The error ranges of the $P(E_T)$ and $T(\theta)$ functions are determined within the 1σ limits of the corresponding laboratory angular distribution.

Electronic Structure Calculations. Geometries of various species (reactants, intermediates, transition states, products) on the C_5H_3 potential energy surface (PES) were optimized using the doubly hybrid DFT B2PLYPD3 method (56–58) with Dunning's correlation-consistent cc-pVTZ basis set (38). The exceptions were intermediate **i1** and the transition state connecting **i1** and **i2**, which could not be found at the B2PLYPD3/cc-pVTZ level of theory; these were located using hybrid DFT B3LYP/cc-pVTZ calculations. Vibrational frequencies were computed at the same levels as geometry optimization, that is, B2PLYPD3/cc-pVTZ for most structures and B3LYP/cc-pVTZ for **i1** and the aforementioned transition state. Single-point energies of the optimized structures were refined using the explicitly correlated coupled clusters CCSD(T)-F12/cc-pVTZ-f12 method (33, 34) to approximate the CCSD(T)/CBS values, that is, the energies within the coupled clusters theory with single and double excitations with perturbative treatment of triple excitations

extrapolated to the complete basis set limit. The accuracy of the CCSD(T)-F12/cc-pVTZ-f12//B2PLYPD3/cc-pVTZ + ZPE (B2PLYPD3/cc-pVTZ) relative energies is expected to be better than 4 kJ·mol⁻¹. Zhang and Valeev (59) showed for a typical set of chemical reactions that the mean absolute errors in CCSD(T)-F12/cc-pVTZ-f12-calculated reaction energies and barrier heights are 2.3 and 1.2 kJ·mol⁻¹, with the maximal absolute errors being 6.4 and 3.3 kJ·mol⁻¹, respectively. A presence of a multireference character in the wavefunctions was monitored by the T1 diagnostic values from CCSD calculations. It appeared that T1 diagnostics exceeded 0.03 for **i1**, the transition state, and for several structures along the minimal energy paths (MEP) for the H losses from **i2** to **p1** and from **i3** to **p2** occurring without exit barriers, which were utilized in variational transition state theory calculations of rate constants of the corresponding reaction steps (discussed below). For these structures, the wavefunctions are likely to exhibit a significant multireference character making the CCSD(T)-F12 energies less reliable. Therefore, their single point energies were instead refined using a multireference perturbation theory CASPT2 approach (37) with active space including 13 electrons distributed on 10 orbitals and with the cc-pVTZ basis set. To circumvent the lack of size consistency for the CASPT2 method, the CASPT2(13, 10)/cc-pVTZ relative energies of **i1** and the transition state were computed with respect to a "supermolecule" made from the reactants at a large separation where their interaction is negligible, whereas those for the **i2-p1** and **i3-p2** MEP structures were evaluated with respect to the decomposing **i2** and **i3** intermediates, respectively. The B3LYP and B2PLYPD3 calculations were performed using the Gaussian 09 (60) software package, whereas the CCSD(T)-F12 and CASPT2 calculations were performed using Molpro 2010 (61).

RRKM theory (41) was used to compute energy-dependent rate constants of all unimolecular reaction steps on the C₃H₃ PES following the initial association of the methylidyne radical with diacetylene and to evaluate product branching ratios under single-collision conditions. For the hydrogen atom elimination reaction steps occurring without exit barriers, microcanonical variational transition state theory (μ -VTST) (41) was employed. The data required for μ -VTST calculations include optimized geometries, vibrational frequencies, and refined single-point energies for a series of structures on the respective hydrogen atom loss path. These data were computed either at our regular CCSD(T)-F12/cc-pVTZ-f12//B2PLYPD3/cc-pVTZ level or at the CASPT2(13, 10)/cc-pVTZ//B3LYP/cc-pVTZ level for the **i2-p1** and **i3-p2** paths where several structures showed a significant multireference character. More detail on our approach to conventional RRKM and variational transition state theory energy-dependent calculations are provided in an earlier publication (62), but here we employed our recently developed in-house Unimol software code (63) to generate all rate constants and product branching ratios depending on the collision energy.

Molecular Dynamics Calculations. The AIMD simulations are carried out with a combined software package of NWChem (v6.3) (64) and VENUS (65). The energy gradients are calculated in NWChem, which are passed to VENUS to solve the classical equations of motion to propagate the trajectories (66). At the beginning of the simulation, the reactant molecules are separated by 1,200 PM, thus minimizing any intermolecular interaction between them; the reactants collide at a collision energy of 19.4 kJ·mol⁻¹ at a fixed impact parameter *b*. To match the experimental conditions, the initial vibrational and rotational energies for diacetylene (C₄H₂) are selected from a canonical ensemble at 15 K, while the methylidyne radical is defined by its vibrational

ground state and a rotational temperature of 14 K. The time step of the AIMD simulations is 0.2 fs. The trajectories are halted once the products are formed or they go back to the reactants after the collision. The simulations start from *b* = 100 PM; larger impact parameters are sampled with an increment of 100 PM until no reactive trajectories are found, for example 0 out of 250 reactive trajectories at *b* = 500 PM. The number of trajectories simulated at each *b* value is proportional to the probability of collision, that is, 100, 200, 300, and 400 trajectories for *b* at 100 PM, 200 PM, 300 PM, and 400 PM, respectively. Over this range of impact parameters, the probability of reaction, *P*(*b*), decreases from 5 to less than 1%.

The quantum chemistry method employed in the AIMD simulations should represent the potential energies of this reaction accurately. Further, an AIMD simulation involves millions of energy gradient calculations to propagate the trajectory, and thus the quantum chemistry method also needs to be computationally efficient. Here, the potential energy profile is computed at the CCSD(T)-F12/cc-pVQZ-f12//B2PLYPD3/cc-pVTZ level of theory (34, 38, 58, 67), which serves as the benchmark to evaluate the performance of a series of affordable methods such as MP2 and DFTs combined with double-zeta basis sets (SI Appendix, Table S3). The root mean square displacement (RMSD) between the benchmark and the potential energies from candidate quantum chemistry methods are computed with Eq. 1 (68–70):

$$RMSD = \sqrt{\frac{1}{N} \sum_{i=1}^N \delta_i^2}, \quad \delta_i = PE(i) - PE_{ref}(i), \quad [1]$$

in which δ_i is the difference in relative potential energy between the benchmark value and the value calculated from candidate method and *N* is the total number of key points on the potential energy profile, including the reactants, intermediates, transition states, and products. In addition to locating all key points involved in this reaction, the quantum chemistry method should be stable in handling nonoptimal structures and conserve the total energy of the system. This feature is often overlooked but is of particular importance in simulating the present reaction: As shown in section *Electronic Structure Calculations*, the entrance channel reveals high multireference character, which is known to cause numerous convergences problems to candidate quantum chemistry methods listed in SI Appendix, Table S3. Therefore, those methods (SI Appendix, Table S3) with low RMSD values have been employed to test their stability in AIMD simulations. Although B3LYP with the two Pople basis sets (6-31+G* and 6-311++G**) have slightly lower RMSD (68–70), the total energies of their trajectories are not as stable as with B3LYP/cc-pVDZ (38). Therefore, balancing the concerns of accuracy, feasibility, and stability, B3LYP/cc-pVDZ is chosen to be the quantum chemistry method in the AIMD simulations.

Data Availability. All study data are included in the paper, SI Appendix, and Dataset S1.

ACKNOWLEDGMENTS. This work was supported by the US Department of Energy, Basic Energy Sciences grants DE-FG02-03ER15411 and DE-FG02-04ER15570 to the University of Hawaii and to Florida International University, respectively. The AIMD trajectories are carried out with the advanced computing resources provided by the University of Hawaii Information Technology Service Cyberinfrastructure.

1. P. Thaddeus, J. M. Vrtilek, C. A. Gottlieb, Laboratory and astronomical identification of cyclopropenylidene, C₃H₂. *Astrophys. J.* **299**, L63–L66 (1985).
2. P. Cox, C. M. Walmsley, R. Güsten, C₃H₂ observations in dense dark clouds. *Astron. Astrophys.* **209**, 382–390 (1989).
3. H. P. Reisenauer, G. Maier, A. Riemann, R. W. Hoffmann, Cyclopropenylidene. *Angew. Chem. Int. Ed. Engl.* **23**, 641 (1984).
4. J. Cernicharo *et al.*, Astronomical detection of H₂CCC. *Astrophys. J.* **368**, L39–L41 (1991).
5. G. Maier *et al.*, Vinylidene carbene: A new C₃H₂ species. *J. Am. Chem. Soc.* **109**, 5183–5188 (1987).
6. R. A. Seburt, R. J. McMahon, Automerizations and isomerizations in propynylidene (HCCCH), propadienylidene (H₂CCC), and cyclopropenylidene (c-C₃H₂). *Angew. Chem. Int. Ed. Engl.* **34**, 2009–2012 (1995).
7. R. A. Seburt, J. T. DePinto, E. V. Patterson, R. J. McMahon, Structure of triplet propynylidene. *J. Am. Chem. Soc.* **117**, 835–836 (1995).
8. R. A. Seburt, E. V. Patterson, J. F. Stanton, R. J. McMahon, Structures, automerizations, and isomerizations of C₃H₂ isomers. *J. Am. Chem. Soc.* **119**, 5847–5856 (1997).
9. P. Botschwina, Accurate equilibrium structures for small polyatomic molecules, radicals and carbenes. *Mol. Phys.* **103**, 1441–1460 (2005).
10. R. A. Seburt, R. J. McMahon, J. F. Stanton, J. Gauss, Structures and stabilities of C₃H₂ isomers: Quantum chemical studies. *J. Am. Chem. Soc.* **119**, 10838–10845 (1997).
11. D. L. Cooper, S. C. Murphy, Ab initio geometries for C_{2n+1}H, C_{2n+1}H⁺, and C_{2n+1}H₂ species for *n* = 1, 2, 3. *Astrophys. J.* **333**, 482–490 (1988).
12. V. S. Thimmakonda, I. Ulusoy, A. K. Wilson, A. Karton, Theoretical studies of two key low-lying carbenes of C₅H₂ missing in the laboratory. *J. Phys. Chem. A* **123**, 6618–6627 (2019).
13. J. M. Vrtilek, C. A. Gottlieb, E. W. Gottlieb, T. C. Killian, P. Thaddeus, Laboratory detection of propadienylidene, H₂CCC. *Astrophys. J.* **364**, L53–L56 (1990).
14. R. Herges, A. Mebel, Propargylene. *J. Am. Chem. Soc.* **116**, 8229–8237 (1994).
15. A. M. Mebel, W. M. Jackson, A. H. H. Chang, S. H. Lin, Photodissociation dynamics of propyne and allene: A view from ab initio calculations of the C₃H_{*n*} (*n* = 1–4) species and the isomerization mechanism for C₃H₂. *J. Am. Chem. Soc.* **120**, 5751–5763 (1998).
16. M. C. van Hemert, E. F. van Dishoeck, Photodissociation of small carbonaceous molecules of astrophysical interest. *Chem. Phys.* **343**, 292–302 (2008).
17. A. V. Wilson, D. S. N. Parker, F. Zhang, R. I. Kaiser, Crossed beam study of the atom-radical reaction of ground state carbon atoms (C²P) with the vinyl radical (C₂H₃(X²A')). *Phys. Chem. Chem. Phys.* **14**, 477–481 (2012).
18. P. Maksyutenko, F. Zhang, X. Gu, R. I. Kaiser, A crossed molecular beam study on the reaction of methylidyne radicals [CH(X²I)] with acetylene [C₂H₂(X¹Σ_g⁺)]-competing C₃H₂ + H and C₃H + H₂ channels. *Phys. Chem. Chem. Phys.* **13**, 240–252 (2011).
19. M. C. McCarthy *et al.*, Detection and characterization of the cumulene carbenes H₂C₅ and H₂C₆. *Science* **275**, 518–520 (1997).

20. M. J. Travers, M. C. McCarthy, C. A. Gottlieb, P. Thaddeus, Laboratory detection of the ring-chain molecule C_5H_2 . *Astrophys. J.* **483**, L135–L138 (1997).
21. C. A. Gottlieb *et al.*, Laboratory detection of two new C_5H_2 isomers. *Astrophys. J.* **509**, L141–L144 (1998).
22. M. C. McCarthy, M. J. Travers, A. Kovács, C. A. Gottlieb, P. Thaddeus, Eight new carbon chain molecules. *Astrophys. J. Suppl. Ser.* **113**, 105–120 (1997).
23. M. C. McCarthy, P. Thaddeus, Carbon-13 isotopic species of H_2C_3 , H_2C_4 , and H_2C_5 : High-resolution rotational spectra. *J. Mol. Spectrosc.* **211**, 235–240 (2002).
24. M. Steglich, J. Fulara, S. Maity, A. Nagy, J. P. Maier, Electronic spectra of linear HC_5H and cumulene carbene H_2C_5 . *J. Chem. Phys.* **142**, 244311 (2015).
25. S. A. Maluendes, A. D. McLean, Ab initio predictions on the rotational spectra of carbon-chain carbene molecules. *Chem. Phys. Lett.* **200**, 511–517 (1992).
26. N. P. Bowling *et al.*, Reactive carbon-chain molecules: Synthesis of 1-diazo-2,4-pentadiyne and spectroscopic characterization of triplet pentadiynylidene ($H-CC-C-CC-H$). *J. Am. Chem. Soc.* **128**, 3291–3302 (2006).
27. S. J. Blanksby, S. Dua, J. H. Bowie, D. Schröder, H. Schwarz, Gas-phase syntheses of three isomeric C_5H_2 radical anions and their elusive neutrals: a joint experimental and theoretical study. *J. Phys. Chem. A* **102**, 9949–9956 (1998).
28. E. Reusch *et al.*, Pentadiynylidene and its methyl-substituted derivatives: Threshold photoelectron spectroscopy of $R_1-C_5-R_2$ triplet carbon chains. *J. Phys. Chem. A* **123**, 2008–2017 (2019).
29. A. Balakrishnan, R. Shankar, S. Vijayakumar, Reduced bond length alternation and helical molecular orbitals in donor and acceptor substituted linear carbon chains. *J. Theor. Comput. Chem.* **17**, 1850049 (2018).
30. R. D. Levine, *Molecular Reaction Dynamics* (Cambridge University Press, 2005).
31. W. B. Miller, S. A. Safron, D. R. Herschbach, Exchange reactions of alkali atoms with alkali halides: A collision complex mechanism. *Discuss. Faraday Soc.* **44**, 108–122 (1967).
32. J. M. Ribeiro, A. M. Mebel, Reaction mechanism and product branching ratios of the $CH + C_3H_4$ reactions: A theoretical study. *Phys. Chem. Chem. Phys.* **19**, 14543–14554 (2017).
33. G. Knizia, T. B. Adler, H.-J. Werner, Simplified CCSD(T)-F12 methods: Theory and benchmarks. *J. Chem. Phys.* **130**, 054104 (2009).
34. T. B. Adler, G. Knizia, H.-J. Werner, A simple and efficient CCSD(T)-F12 approximation. *J. Chem. Phys.* **127**, 221106 (2007).
35. K. A. Peterson, D. E. Woon, T. H. Dunning Jr, Benchmark calculations with correlated molecular wave functions. IV. The classical barrier height of the $H + H_2 \rightarrow H_2 + H$ reaction. *J. Chem. Phys.* **100**, 7410–7415 (1994).
36. A. D. Becke, Density functional thermochemistry. III. The role of exact exchange. *J. Chem. Phys.* **98**, 5648–5652 (1993).
37. T. Shiozaki, W. Györfy, P. Celani, H.-J. Werner, Communication: Extended multi-state complete active space second-order perturbation theory: Energy and nuclear gradients. *J. Chem. Phys.* **135**, 081106 (2011).
38. T. H. Dunning Jr, Gaussian basis sets for use in correlated molecular calculations. I. The atoms Boron through Neon and Hydrogen. *J. Chem. Phys.* **90**, 1007–1023 (1989).
39. H. Kayi, P. Garcia-Fernandez, I. B. Bersuker, J. E. Boggs, Deviations from Born-Oppenheimer theory in structural chemistry: Jahn-Teller, pseudo Jahn-Teller, and hidden pseudo Jahn-Teller effects in C_3H_3 and $C_3H_3^-$. *J. Phys. Chem. A* **117**, 8671–8679 (2013).
40. J. G. López *et al.*, A direct dynamics trajectory study of $F + CH_3OOH$ reactive collisions reveals a major non-IRC reaction path. *J. Am. Chem. Soc.* **129**, 9976–9985 (2007).
41. J. I. Steinfeld, J. S. Francisco, W. L. Hase, *Chemical Kinetics and Dynamics* (Prentice Hall, Englewood Cliffs, 1982).
42. A. M. Mebel, S. H. Lin, X. M. Yang, Y. T. Lee, Theoretical study on the mechanism of the dissociation of benzene. the $C_5H_3 + CH_3$ product channel. *J. Phys. Chem. A* **101**, 6781–6789 (1997).
43. C. J. Pope, J. A. Miller, Exploring old and new benzene formation pathways in low-pressure premixed flames of aliphatic fuels. *Proc. Combust. Inst.* **28**, 1519–1527 (2000).
44. M. S. Skjøth-Rasmussen *et al.*, A study of benzene formation in a laminar flow reactor. *Proc. Combust. Inst.* **29**, 1329–1336 (2002).
45. J. Cernicharo *et al.*, Infrared space observatory's discovery of C_4H_2 , C_6H_2 , and benzene in CRL 618. *Astrophys. J.* **546**, L123–L126 (2001).
46. N. Hansen *et al.*, A combined ab initio and photoionization mass spectrometric study of polyynes in fuel-rich flames. *Phys. Chem. Chem. Phys.* **10**, 366–374 (2008).
47. S. Chandra, S. A. Shinde, Suggestions for an interstellar C_5H_2 search. *Astron. Astrophys.* **423**, 235–239 (2004).
48. M. C. McCarthy, M. J. Travers, C. A. Gottlieb, P. Thaddeus, Laboratory detection of the ring-chain molecule C_7H_2 . *Astrophys. J.* **483**, L139–L142 (1997).
49. A. J. Apponi, M. C. McCarthy, C. A. Gottlieb, P. Thaddeus, Laboratory detection of four new cumulene carbenes: H_2C_7 , H_2C_8 , H_2C_9 , and D_2C_{10} . *Astrophys. J.* **530**, 357–361 (2000).
50. C. D. Ball, M. C. McCarthy, P. Thaddeus, Cavity ringdown spectroscopy of the linear carbon chains HC_7H , HC_9H , $HC_{11}H$, and $HC_{13}H$. *J. Chem. Phys.* **112**, 10149–10155 (2000).
51. S. Dua, S. J. Blanksby, J. H. Bowie, The syntheses of $C_6CH_2^-$ and the corresponding carbenoid cumulene C_6CH_2 in the gas phase. *Chem. Commun. (Camb.)* 1767–1768 (1998).
52. C. D. Ball, M. C. McCarthy, P. Thaddeus, Laser spectroscopy of the carbon chains HC_7H and HC_9H . *Astrophys. J.* **523**, L89–L91 (1999).
53. R. I. Kaiser *et al.*, Untangling the chemical evolution of Titan's atmosphere and surface—from homogeneous to heterogeneous chemistry. *Faraday Discuss.* **147**, 429–478, discussion 527–552 (2010).
54. F. Zhang, P. Maksyutenko, R. I. Kaiser, Chemical dynamics of the $CH(X^2\Pi) + C_2H_4(X^1A_{1g})$, $CH(X^2\Pi) + C_2D_4(X^1A_{1g})$, and $CD(X^2\Pi) + C_2H_4(X^1A_{1g})$ reactions studied under single collision conditions. *Phys. Chem. Chem. Phys.* **14**, 529–537 (2012).
55. F. Zhang, S. Kim, R. I. Kaiser, A. M. Mebel, Formation of the 1,3,5-hexatriynyl radical ($C_6H(X^2\Pi)$) via the crossed beams reaction of dicarbon ($C_2(X^1\Sigma_g^+/a^3\Pi_u)$) with diacetylene ($C_4H_2(X^1\Sigma_g^+)$). *J. Phys. Chem. A* **113**, 1210–1217 (2009).
56. S. Grimme, S. Ehrlich, L. Goerigk, Effect of the damping function in dispersion corrected density functional theory. *J. Comput. Chem.* **32**, 1456–1465 (2011).
57. L. Goerigk, S. Grimme, Efficient and accurate Double-Hybrid-Meta-GGA density functionals-evaluation with the extended GMTKN30 database for general main group thermochemistry, kinetics, and noncovalent interactions. *J. Chem. Theory Comput.* **7**, 291–309 (2011).
58. S. Grimme, Semiempirical hybrid density functional with perturbative second-order correlation. *J. Chem. Phys.* **124**, 034108 (2006).
59. J. Zhang, E. F. Valeev, Prediction of reaction barriers and thermochemical properties with explicitly correlated coupled-cluster methods: A basis set assessment. *J. Chem. Theory Comput.* **8**, 3175–3186 (2012).
60. M. J. Frisch *et al.*, Gaussian 09, revision D. 01, Gaussian (Gaussian Inc., Wallingford, CT, 2009).
61. H. J. Werner *et al.*, MOLPRO, a package of ab initio programs (Version 2010.1, University of Cardiff, Cardiff, UK, 2010).
62. V. V. Kislov, T. L. Nguyen, A. M. Mebel, S. H. Lin, S. C. Smith, Photodissociation of benzene under collision-free conditions: An ab initio/rice-ramsperger-kassel-marcus study. *J. Chem. Phys.* **120**, 7008–7017 (2004).
63. C. He *et al.*, Elucidating the chemical dynamics of the elementary reactions of the 1-propynyl radical (CH_3CC ; X^2A_1) with methylacetylene (H_3CCCH ; X^1A_1) and allene (H_2CCCH_2 ; X^1A_1). *J. Phys. Chem. A* **123**, 5446–5462 (2019).
64. M. Valiev *et al.*, NWChem: A comprehensive and scalable open-source solution for large scale molecular simulations. *Comput. Phys. Commun.* **181**, 1477–1489 (2010).
65. X. Hu, W. L. Hase, T. Pirraglia, Vectorization of the general Monte Carlo classical trajectory program VENUS. *J. Comput. Chem.* **12**, 1014–1024 (1991).
66. U. Lourderaj *et al.*, The VENUS/NWChem software package. Tight coupling between chemical dynamics simulations and electronic structure theory. *Comput. Phys. Commun.* **185**, 1074–1080 (2014).
67. K. A. Peterson, T. B. Adler, H.-J. Werner, Systematically convergent basis sets for explicitly correlated wavefunctions: The atoms H, He, B-Ne, and Al-Ar. *J. Chem. Phys.* **128**, 084102 (2008).
68. W. Kabsch, A solution for the best rotation to relate two sets of vectors. *Acta Crystallogr. A* **32**, 922–923 (1976).
69. A. D. McLachlan, A mathematical procedure for superimposing atomic coordinates of proteins. *Acta Crystallogr. A* **28**, 656–657 (1972).
70. A. Kuzmanic, B. Zagrovic, Determination of ensemble-average pairwise root mean-square deviation from experimental B-factors. *Biophys. J.* **98**, 861–871 (2010).